

Finite Element Model to Study the Thermal Effect of Tumor in Human Head

Mona Dwivedi¹, Usha Chouhan²

¹(Department of Mathematics, Maulana Azad National Institute of Technology, Bhopal, M.P., India-462051)

²(Department of Mathematics, Maulana Azad National Institute of Technology, Bhopal, M.P., India-462051)

Abstract: *The temperature distribution in human head regulate variety of biological mechanism. Human head is a very complex structure and abnormality in temperature of various layer of human head play important role for treatment of diseases like tumor, cancer, hyperthermia, hypothermia etc. Here, a finite element model has been developed to study the temperature distribution of human head with ten layers namely brain, skull, fat-layer, reticular region, papillary region, stratum germinativum, stratum spinosum, stratum granulosum, stratum lucidum and stratum corneum in presence of tumor in the reticular region. Appropriate boundary conditions have been framed and finite element method is used to obtain temperature values in one dimension. A program is developed on MATLAB for simulation of results. The numerical results have been used to study the effect on temperature variation in cold environment on normal tissue and in presence of tumor in reticular region of human head.*

Keywords - *Temperature Distribution, Blood mass flow rate, Finite Element Method,*

I. Introduction

The thermal imbalance in human head due to strong heating and extreme cooling causes many diseases like head trauma, stroke, multiple sclerosis [1]. The cold injury in human body is called frostbite and the cold exposure is called hypothermia [2]. Hypothermia has therapeutic roles in many clinical conditions like anoxic brain injury due to cardiac arrest, head trauma and hypoxic ischemic neonatal encephalopathy [3, 4]. The phenomenon of lowering the temperature of human body core temperature below 35°C is known as hypothermia [5]. The effect of cold exposure in human body is reflected in terms of decreasing biochemical reactions, muscle fatigue, increasing blood pressure and bronchoconstriction. The human head is very sensitive to surrounding temperature [5, 6]. The thermal receptors located in dermis pass the environmental information to the hypothalamus center in the head. The nervous communication is activated to renew rate of blood supply and other processes to counter the cold effect [6]. Actually, a small temperature increase in the human head of 3.5°C is noted to be an allowable limit which does not lead to physiological damage [7]. Additionally, it is reported that a very small temperature increase in the hypothalamus of 0.2-0.3°C leads to altered thermoregulatory behavior [7]. Hyperthermia has been used in the evaluation of patients suspected of having tumor, where an abnormal thermal pattern can be detected prior to clinical changes. Hyperthermia tumor treatment has proven to be an effective method in tumor treatment compare to surgery, chemotherapy and radiation. In Hyperthermia tumor treatment involves heating a tumor region to 43°C to 45°C [8]. Even though this temperature is unpleasant for the patient, tumor cells are more susceptible to this temperature range and can be killed over a period of time. These methods cause minimal damage to the healthy tissue therefore leaving limited negative side effects in this treatment [8]. Although a high temperature is required in tumor region but the conditions of "partial body exposure" to intense heating beyond the hyperthermia may cause some serious thermal damage to human body [9]. Human body tissues have different values of dielectric properties, that is, permittivity and conductivity [9]. These properties are functions of many variables like frequency, geometry, size of tissue and water contents [10]. The head is the most important organ of the human body. Human head control the whole body and any abnormality regarding to thermoregulation processes in it cause improper functioning not only in brain tissue but also to the rest of the body [2]. The adverse modification in brain tissue temperature leads in cerebral metabolism, dysfunction of the central nervous and endocrine system [2, 11]. We propose that one possible way to analyze this is to compute the effect of different body heat transfer mechanisms on the human brain [12]. The major mechanisms contributing to brain temperature regulation are metabolic heat production, heat removal by blood flow, heat conductance and heat exchange with the environment. The balance between these factors defines temperature distribution in the brain. Severely cold environment causes variations in the regional blood flow and metabolic processes. Thus study of temperature variation in brain is more interesting at lower atmospheric temperature [8, 13]. In this paper the temperature of human brain is assumed to be equal to the core temperature of body (37°C) and effects of low atmospheric temperature on tumor are

studied. Different types of variations of parameters have been considered for different natural subregions such as skull, fat-layer, reticular region, papillary region, stratum germinativum, stratum spinosum, stratum granulosum, stratum lucidum and stratum corneum.

II. Mathematical Model

The domain of head is considered as a system consisting of cerebral tissue (brain) with overlaying layers of skull, fat-layer, reticular region, papillary region, stratum germinativum, stratum spinosum, stratum granulosum, stratum lucidum and stratum corneum. The distribution of heat in tissues is given by Pennes equation [12, 13, 14]

$$\rho c \frac{\partial T}{\partial t} = \nabla(K \cdot \nabla T) + c_b \rho_b \omega_m (T_A - T) + Q_m \quad (1)$$

Here ρ, c and K are the tissue density, specific heat, and thermal conductivity of tissue, respectively, c_b is the specific heat of blood, ρ_b is the density of blood, T is the tissue temperature, T_A is the arterial blood temperature, t is the time, Q_m is the metabolic heat generation rate per unit volume and ω_m is the blood perfusion rate. The outer surface of the skin is exposed to the environment and the heat loss from the outer skin surface to the environment takes place by conduction, convection, radiation and evaporation. Therefore, the boundary condition at the outer surface can be written as [2, 6, 13]

$$-K \frac{\partial T}{\partial \eta} = h(T - T_a) + LE \quad x = l_0 \quad (2)$$

Where h is the heat transfer coefficient and η is the unit direction normal to the surface boundary, T_a is the temperature of the surrounding atmosphere, L is the latent heat of evaporation and E is the rate of sweat evaporation. The inner brain core temperature T_b is assumed to be $37^\circ C$. Therefore, the inner boundary condition is prescribed as given below

$$T(x = l_{10}, t) = T_b \quad (3)$$

Where T_b the body core temperature and l_{10} is the thickness of the human head. Also at the interfaces between adjoining layers, we have [2]

$$\begin{aligned} T_i &= T_{i+1} \\ \text{and} & \\ \left(K \frac{\partial T}{\partial \eta} \right)_i &= \left(K \frac{\partial T}{\partial \eta} \right)_{(i+1)} \end{aligned} \quad (4)$$

The equation (4) represents the continuity of temperature and heat flux between different sub domains of the region under study. It is also assumed that at time $t = 0$ all layers of the human head having temperature $37^\circ C$. Thus, the initial condition is given by

$$T(x, 0) = 37^\circ C \quad (5)$$

The layer of different parts of the human head is show in the Figure 1. The thickness of stratum corneum, stratum lucidum, stratum granulosum, stratum spinosum, stratum germinativum, papillary region, reticular region, fat-layer, skull and brain tissue layers have been considered as $l_1, (l_2 - l_1), (l_3 - l_2), (l_4 - l_3), (l_5 - l_4), (l_6 - l_5), (l_7 - l_6), (l_8 - l_7), (l_9 - l_8)$ and $(l_{10} - l_9)$ respectively and $T_0, T_1, T_2, T_3, T_4, T_5, T_6, T_7, T_8, T_9$ and T_{10} are the nodal temperatures at a distances $x = l_0, x = l_1, x = l_2, x = l_3, x = l_4, x = l_5, x = l_6, x = l_7, x = l_8, x = l_9$ and $x = l_{10}$ and $T^{(i)}$ for $i = 1, 2, 3, 4, 5, 6, 7, 8, 9,$ and 10 represents the temperature functions in the layers stratum corneum, stratum lucidum, stratum granulosum, stratum spinosum, stratum germinativum (basale), papillary region, reticular region, fat-layer, skull and brain tissue respectively.

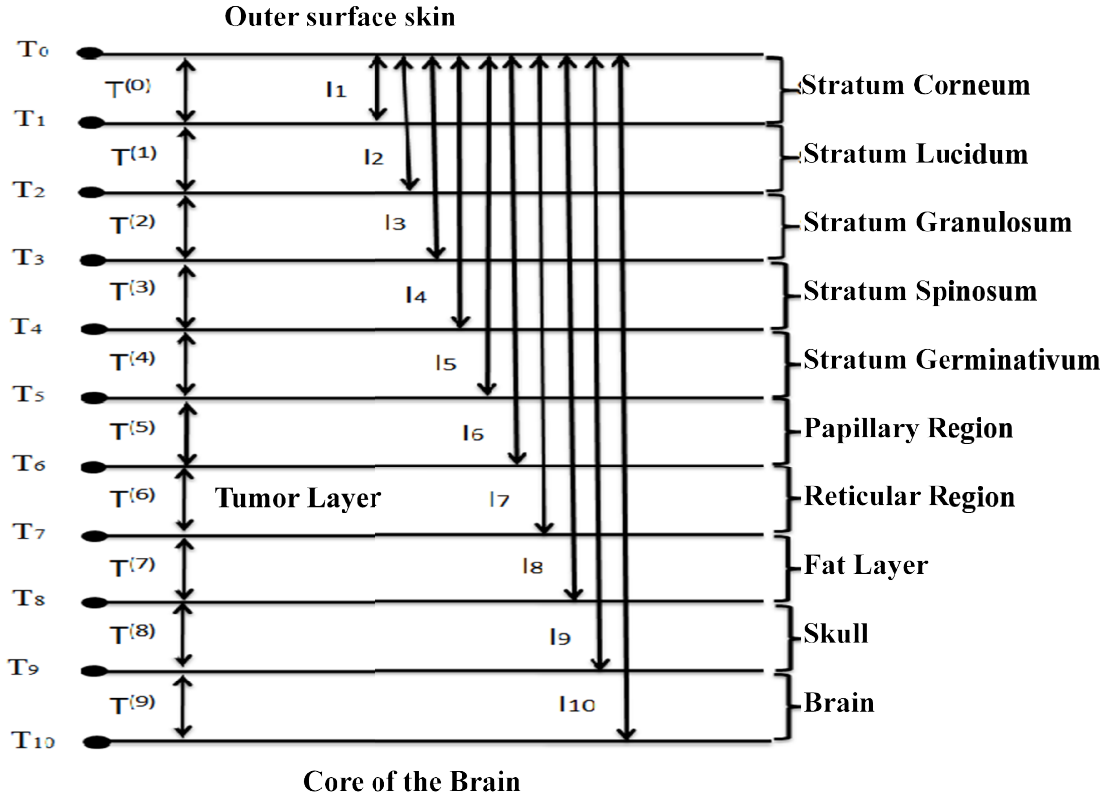


Figure 1. Ten Layer Model of Human Head with Tumor in the Reticular Region

The discretized variational form of equation (1) to (4) can be written as follows:

$$I^{(e)} = \frac{1}{2} \int_{l_{(e-1)}}^{l_e} \left[K \left(\frac{\partial T}{\partial x} \right)^2 + M (T_A - T)^2 - 2Q_m T + \rho c \frac{\partial T^2}{\partial t} \right] dx + \frac{\mu^{(e)}}{2} \{ h(T - T_a)^2 + 2LET^{(e)} \} \quad \text{for } e = 1, 2, \dots, 10. \tag{6}$$

Here $M = c_b \rho_b \omega_m$, e denotes the element number and $\mu^{(e)} = 1$ for $e=1$ i.e., the elements near the outer surface and $\mu^{(e)} = 0$ for other elements. The following linear shape function for variation of temperature within each element has been taken as:

$$T^{(e)} = c_1^{(e)} + c_2^{(e)} x \tag{7}$$

Where $c_1^{(e)}$ and $c_2^{(e)}$ are constant for the e^{th} element. The equation (7) can be rewritten as

$$T^{(e)} = p^T c^{(e)} \tag{8}$$

where

$$p^T = [1 \quad x] \tag{9}$$

and

$$[c^{(e)}]^T = [c_1^{(e)} \quad c_2^{(e)}] \tag{10}$$

Substituting nodal conditions in equation (7), we get

$$\bar{T}^{(e)} = P^{(e)} * c^{(e)} \tag{11}$$

where

$$\bar{T}^{(e)} = \begin{bmatrix} T_i \\ T_j \end{bmatrix} \quad \text{and} \quad P^{(e)} = \begin{bmatrix} 1 & x_i \\ 1 & x_j \end{bmatrix} \tag{12}$$

From the equation (10), we have

$$c^{(e)} = R^{(e)} * \bar{T}^{(e)} \tag{13}$$

where

$$R^{(e)} = P^{(e)-1} \tag{14}$$

Substituting $c^{(e)}$ from equation (12) in (7), we get

$$T^{(e)} = p^T R^{(e)} \bar{T}^{(e)} \tag{15}$$

Now the integral $I^{(e)}$ can be written in the form

$$I^{(e)} = I_t^{(e)} + I_k^{(e)} + I_m^{(e)} - I_s^{(e)} - \psi^{(e)} I_h^{(e)} \tag{16}$$

where

$$I_t^{(e)} = \frac{1}{2K} \frac{d}{dt} \int_{l_{(e-1)}}^{l_e} \left[(T^{(e)})^2 \right] dx \tag{17}$$

$$I_k^{(e)} = \frac{1}{2} \int_{l_{(e-1)}}^{l_e} \left[\left(\frac{\partial T^{(e)}}{\partial x} \right)^2 \right] dx \tag{18}$$

$$I_m^{(e)} = \frac{1}{2K} \int_{l_{(e-1)}}^{l_e} \left[(T^{(e)})^2 \right] dx \tag{19}$$

$$I_s^{(e)} = \frac{1}{2K} \int_{l_{(e-1)}}^{l_e} \left[2T^{(e)} T_A \right] dx \tag{20}$$

$$I_h = \frac{\psi^{(e)}}{2K} [h(T^{(e)} - T_a)^2 + 2LET^{(e)}] \tag{21}$$

Here $\psi^{(e)} = 1$ for $e=1$, represents the locations/elements of the element near to outer surface of skin and $\psi^{(e)} = 0$ for other elements. The integrals $I^{(e)}$ are evaluated and assembled to obtain I as:

$$I = \sum_{e=1}^{10} \bar{M}^{(e)} I^{(e)} \bar{M}^{(e)T} \tag{22}$$

Now we extremize I w.r.t. each nodal temperature value T_i as given below

$$\frac{dI}{d\bar{T}} = \sum_{e=1}^{10} \bar{M}^{(e)} \frac{dI^{(e)}}{d\bar{T}^{(e)}} \bar{M}^{(e)T} \tag{23}$$

where

$$\bar{M}^{(e)} = \begin{bmatrix} 0 & 0 \\ \cdot & \cdot \\ 1 & 0 \\ 0 & 1 \\ \cdot & \cdot \\ 0 & 0 \end{bmatrix}_{1 \times 2}, \bar{T} = \begin{bmatrix} T_0 \\ T_2 \\ \cdot \\ \cdot \\ T_{10} \end{bmatrix}_{1 \times 1} \tag{24}$$

and

$$\frac{dI^{(e)}}{d\bar{T}^{(e)}} = \frac{d}{dt} \frac{dI_t^{(e)}}{d\bar{T}^{(e)}} + \frac{dI_k^{(e)}}{d\bar{T}^{(e)}} + \frac{dI_m^{(e)}}{d\bar{T}^{(e)}} - \frac{dI_s^{(e)}}{d\bar{T}^{(e)}} - \psi^{(e)} \frac{dI_h^{(e)}}{d\bar{T}^{(e)}} \tag{25}$$

This leads to a following system of ordinary differential equation.

$$[M]_{11 \times 11} [\dot{\bar{T}}]_{11 \times 1} + [K]_{11 \times 11} [\bar{T}]_{11 \times 1} = [F]_{11 \times 1} \tag{26}$$

Here, $\bar{T} = [T_0 \ T_2 \ T_3 \ \dots T_{10}]^T$, M and K are system matrices, and F is system vector. The Crank-Nicolson Method is employed to solve the system of equations (26). The time step is taken as 0.001 sec. A computer program in MATLAB 7.11 is developed to find numerical solution to the entire problem.

III. Result And Discussion

In this section, we have shown the numerical results for temperature profile against different biophysical parameters which have been obtained using values of parameters given in Table 1 unless stated along with figures. The constant $l_i (i = 0(1)10)$ can be assigned any value depending upon particular sample of tissue layers under study. The result are computed for the following sample of values of l_i for different layers in mm from the outer surface of the skin of human head to the core of the brain[16,17,18,]

$$l_0=0, \quad l_1=0.02, \quad l_2=0.04, \quad l_3=0.06, \quad l_4=0.08, \quad l_5=0.2, \quad l_6=1.2, \quad l_7=2.2, \quad l_8=5.2, \quad l_9=10.2, \quad l_{10}=88.2$$

Table 1 Thermo-physical parameters[2,6,13,14,15, 19,20,21,22,23,24]

Parameter	Symbol	Value	Unit
Thermal conductivity of normal tissue	K	0.2	Wm ⁻¹ K ⁻¹
Density of blood	ρ_b	1000	Kg m ⁻³
Specific heat blood	c_b	4186	Jkg ⁻¹ K ⁻¹
Blood perfusion rate in normal tissue	w_b	5.4×10^{-3}	s ⁻¹
Arterial blood temperature	T_A	310.15	K
Specific heat of normal tissue	C	3600	Jkg ⁻¹ K ⁻¹
Density of normal tissue	ρ	1200	Kg m ⁻³
Thermal conductivity in tumor region	K_{tumor}	0.5	Wm ⁻¹ K ⁻¹
Density of tumor region	ρ_{tumor}	1050	Kg m ⁻³
Specific heat in tumor region	c_{tumor}	3600	Jkg ⁻¹ K ⁻¹
Blood perfusion rate in tumor region	w_{tumor}	6×10^{-3}	s ⁻¹
Metabolism	Q_m	700	Wm ⁻³
Heat transfer coefficient	H	10	Wm ⁻² K ⁻¹

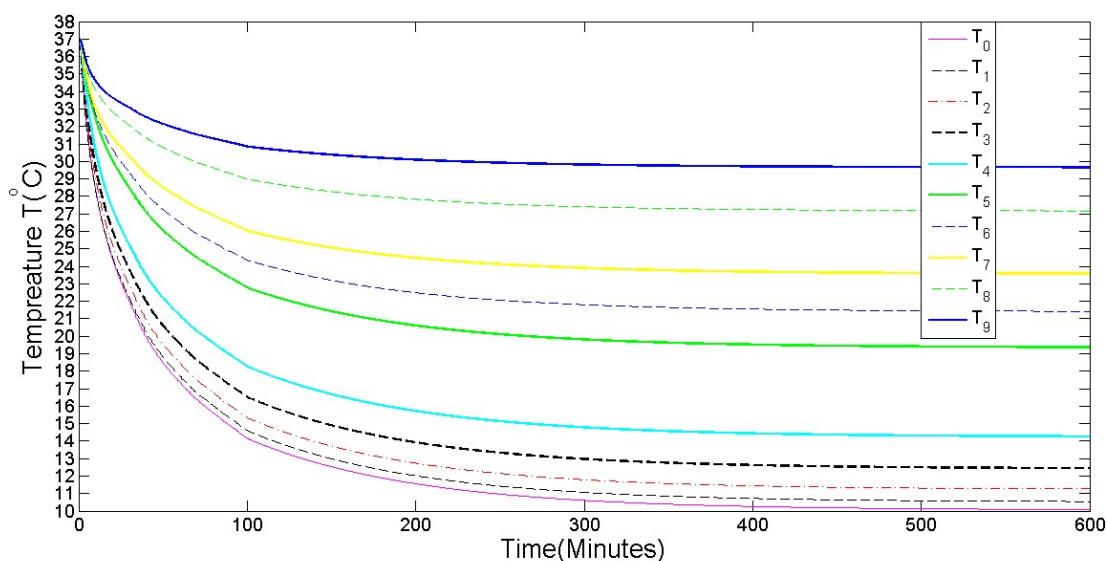


Figure 2. Temperature Distribution in Human Head for 10°C atmospheric temperature when tumor is not present in Reticular Region

Figure 2 shows the temporal temperature distribution at different nodal position in human head for 10°C external environment temperature. The temperature curves indicate that the temperature at the nodal

position T_{10} have higher values than temperature at the nodal position T_0 . This indicates that at 10°C external environment temperature the neighboring region of brain core maintains higher temperature as compared to the neighboring region of external surface.

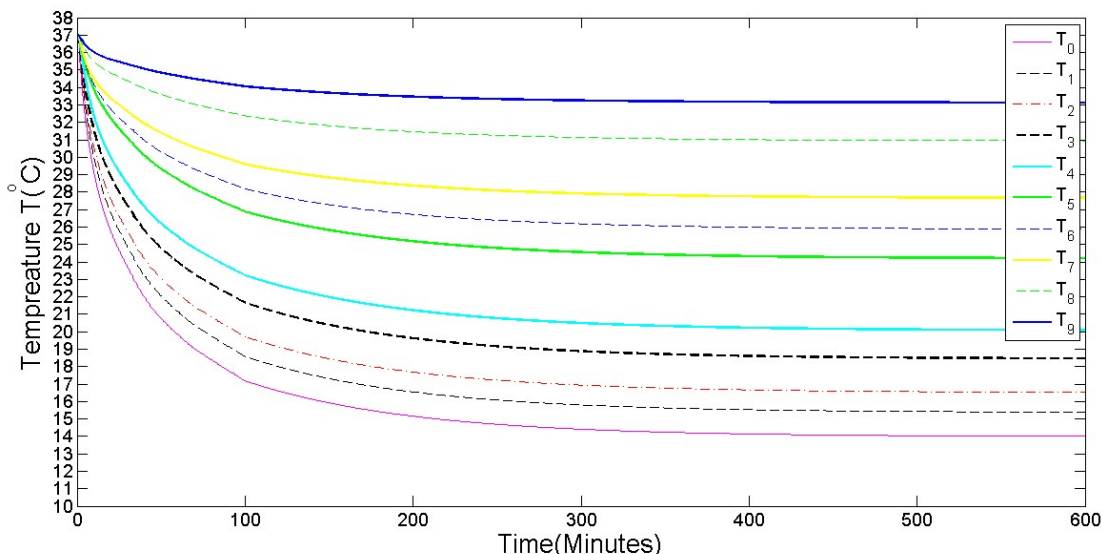


Figure 3. Temperature Distribution in Human Head for 14°C atmospheric temperature when tumor is not present in Reticular Region

Figure 3 shows the temporal temperature distribution at different nodal position in human head for 14°C external environment temperature. Comparing Figure 3 with Figure 2, we observe that the temperature increase at all nodes as the external environment temperature increases.

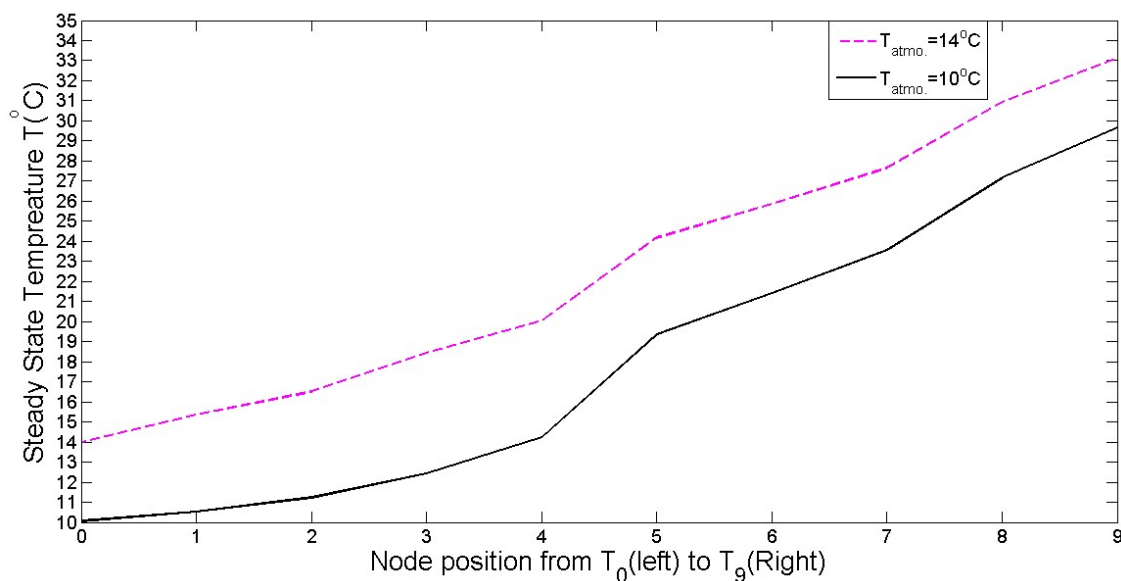


Figure 4. Steady State Nodal Temperature Distribution for two different atmospheric temperature 10°C (Black) and 14°C (Magenta) when tumor is not present at the reticular region

Figure 4 shows the temperature distribution in space for two different values of atmospheric temperature. In figure 4, we observed that the temperature falls down gradually from node T_9 (33°C) to node T_5 (24°C) and then shows a sharp fall from node T_5 (24°C) to T_4 (19.5°C) and then finally achieves 14°C at node T_0 on curve for atmospheric temperature 14°C . Similar behavior is observed on the curve for atmospheric temperature 10°C .

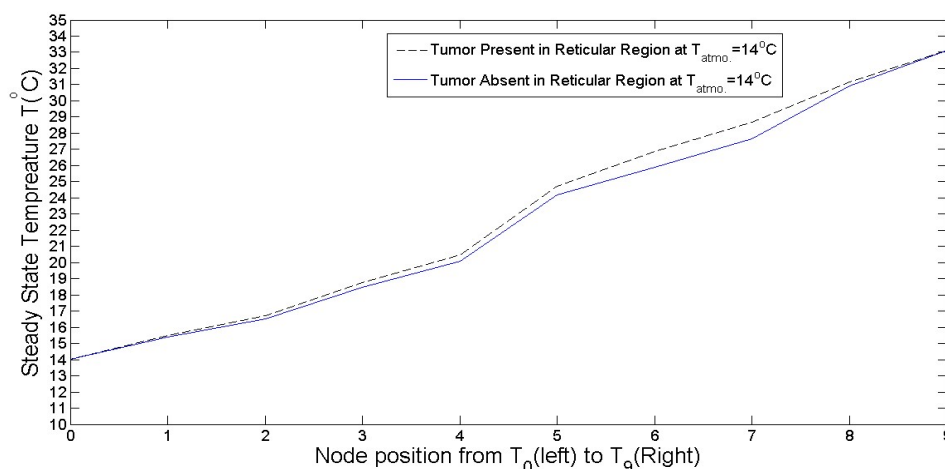


Figure 5. Steady State Nodal Temperature Distribution at atmospheric temperature 14°C when tumor is present at the reticular region (Black) and when tumor is not present in the reticular region (Magenta)

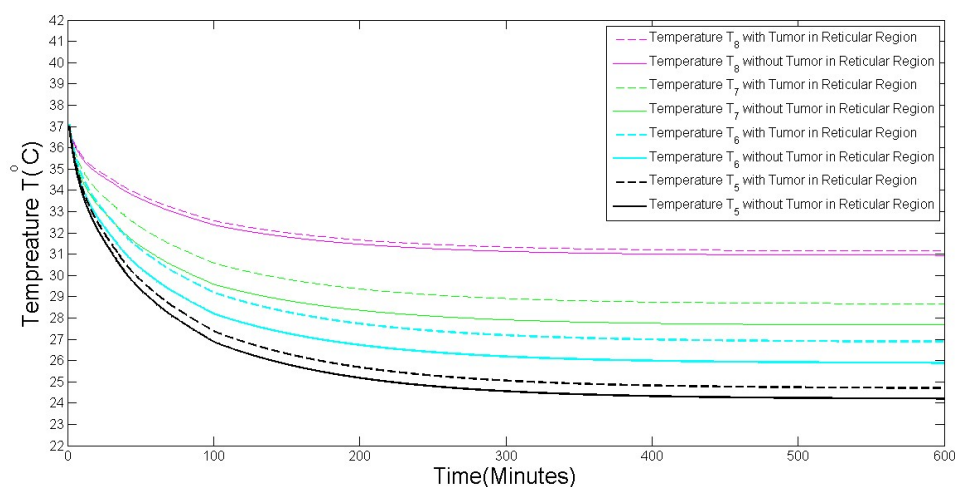


Figure 6. Temporal Temperature Distribution in presence (dotted lines) and absence (Continuous Line) of Tumor in Reticular Region at four different Nodal positions

From Figure 5 and Figure 6, an elevation in temperature profiles (broken lines) is observed towards the reticular region layer due to the presence of tumor in the reticular region. This elevation is very small in the brain and skull layer but increases as we move towards the tumor in the reticular region. The elevation in temperature profiles is more in the reticular region, papillary region and stratum germinativum layer as compared to that in the fat, skull and brain layer. The results agree with the physiological facts like those reported by other researchers [2 6 13]. The variation in the slope of the curves within the limits of maximum thermal disturbances enables us to determine the position and size of the tumor.

IV. Conclusion

The mathematical model study the effect of local hypothermic stress on normal and tumor tissues in different layers of human head using bioheat equation. The approach is seminumerical in nature for temperature distribution in different layers of human head for one-dimensional unsteady-state case. Our model gives better profiles for temperature distribution in brain, skull, fat-layer, reticular region, papillary region, stratum germinativum, stratum spinosum, stratum granulosum, stratum lucidum and stratum corneum. From the present study, information from temperature profiles of normal and tumor tissues can be used to predict the position and size of tumors. Such models can be useful for biomedical scientists to understand the relationship between temperature profiles at different clinical situation.

References

- [1] H. Wang, B Wang, K. P. Normoyle, K. Jackson, K. Spittler, M. F. Sharrock, C. M. Miller, C. Best, D. Llano, and R. Du. "Brain temperature and its fundamental properties: a review for clinical neuroscientists." *Frontiers in neuroscience* 8 (2014).
- [2] M. A. Khanday "Theoretical approach to study the thermal stress on human brain tissue in hypothermic conditions." *Int. J. Adv. Comput. Math. Sci* 4, no. 2: 181-187 (2013).
- [3] S. A. Bernard, T. W. Gray, M. D. Buist, B. M. Jones, W. Silvester, G. Gutteridge, Treatment of comatose survivors of out-of-hospital cardiac arrest with induced hypothermia. *N. Engl. J. Med.* 346, 557–563 10.1056/NEJMoa003289 (2002)
- [4] G. L. Clifton, A. Valadka, D. Zygun, C. S. Coffey, P. Drever, S. Fourwinds, Very early hypothermia induction in patients with severe brain injury (the National Acute Brain Injury Study: Hypothermia II): a randomised trial. *Lancet Neurol.* 10, 131–139 10.1016/S1474-4422(10)70300-8 (2011)
- [5] J. F. Patton, "The Effects of Acute Cold Exposure on Exercise Performance." *The Journal of Strength & Conditioning Research* 2, no. 4: 72-78 (1988).
- [6] M. A. Khanday, V. P. Saxena. "Finite element estimation of one-dimensional unsteady state heat regulation in human head exposed to cold environment." *Journal of Biological systems* 17, no. 04: 853-863 (2009).
- [7] T. Wessapan, P. Rattanadecho, Numerical Analysis of Specific Absorption rate and Heat Transfer in Human Head Subjected to Mobile Phone Radiation: Effects of user Age and Radiated Poser, *Journal of Heat Transfer*, 134: 121101, 9 pages, (2012).
- [8] I. K. Brenner, J. W. Castellani, C. Gabaree, A. J. Young, J. Zamecnik, R. J. Shephard, and P. N. Shek. "Immune changes in humans during cold exposure: effects of prior heating and exercise." *Journal of Applied Physiology* 87, no. 2: 699-710 (1999).
- [9] E. R. Adair, D. R. Black. "Thermoregulatory responses to RF energy absorption." *Bioelectromagnetics* 24, no. S6: S17-S38 (2003).
- [10] A Lak, H Oraizi, Evaluation of SAR Distribution in Six-Layer Human Head Model, *International Journal of Antennas and Propagation*, Hindawi Publishing Corporation, Art ID 580872, 8 pages, (2013).
- [11] S. Mrozek, F.Vardon, T. Geeraerts, "Brain Temperature: Physiology and Pathophysiology after Brain Injury," *Anesthesiology Research and Practice*, vol., Article ID 989487, 13 pages, doi:10.1155/2012/989487 (2012)
- [12] H. H. Pennes, Analysis of tissue and arterial blood temperature in the resting human forearm, *J. Appl. Physiol.*, 1 (1948), 93.
- [13] S. Acharya, D.B. Gurung and V. P. Saxena, Effect of Metabolic Reactions on Thermoregulation in Human Males and Females Body, *Appl. Math.*, 4 39-48 (2013).
- [14] D. D. Rodrigues, P. J. S. Pereira, P. Limao-Vieira, P. R. Stauffer and P. F. Maccarini, Study of the one dimensional and transient bioheat transfer equation: multi-layer solution development and applications, *Int J Heat Mass Transf.*, 62, 153-162, (2013).
- [15] I. Digel, P. Kayser and G. M. Artmann, Molecular Processes in Biological Thermosensation, *Journal of Biophysics*, Hindawi, ID 602870, 9pages, (2008).
- [16] M. H. REpacholi, Low-Level exposure to radiofrequency electromagnetic fields: health effects and research needs, *Bioelectromagnetics*, Vol. 19(1), 20-32, (1998).
- [17] A. G. Pakhomov, Y. Akyel, O. N. Pakhomova, B. E. Stuck and M. R. Murphy, Current state and implications of research on biological effects of millimeter waves: a review of the literature, *Bioelectromagnetics*, 29(7), 393-413, (1998).
- [18] A. C. Guuyton, J. E. Hall, Textbook of Medical physiology, Saunders, Philadelphia, PA, Chap. 73, (1996).
- [19] K. M. Shurrab, M. S. El-Daher, Simulation and Study of Temperature Distribution in Living Biological Tissues under Laser Irradiation. *Journal of lasers in medical sciences*, 5(3), 135-9, (2014).
- [20] S. Hossain, F. A. Mohammadi. "Development Of An Estimation Method For Interior Temperature Distribution In Live Biological Tissues Of Different Organs." *International Journal of Engineering* 3, no. 2 (2013): 8269.
- [21] B. Kumari and N. Adlakha, One Dimensional Model to Study the Effect of Physical Exercise on Temperature Distribution in Peripheral Regions of Human Limbs, *Applied Mathematical Sciences*, 7:1335-1351, (2013).
- [22] E.V. Davydov, I.A. Lubashevsky, V.A. Milyaev, Nondiffusive heat transfer in muscle tissue. Preliminary results. arXiv:cond-mat/0102006 1(1) (2001)
- [23] E. Kengne, A Mathematical Model to Solve Bio-Heat Transfer Problems through a Bio- Heat Transfer Equation with Quadratic Temperature-Dependent Blood Perfusion under a Constant Spatial Heating on Skin Surface. *J. Biomedical Science and Engineering*, 7, 721-730. <http://dx.doi.org/10.4236/jbise.2014.79071> (2014)
- [24] E Kengne, I Mellal, M B Hamouda and A Lakhssassi, A mathematical model to solve Bio-Heat Transfer Problems through a Bio-Heat t5050and N. Ishii, Application of fuzzy theory to writer recognition of Chinese characters, *International Journal of Modelling and Simulation*, 18(2), , 112-116. (8) (1998)